



# The Tec Kinase Itk Integrates Naïve T Cell Migration and *In Vivo* Homeostasis

Flavian Thelen<sup>1</sup>, Stefanie Wissmann<sup>2</sup>, Nora Ruef<sup>2</sup> and Jens V. Stein<sup>2\*</sup>

<sup>1</sup> Department of Medical Oncology and Hematology, University of Zürich and University Hospital Zürich, Zürich, Switzerland,

<sup>2</sup> Department of Oncology, Microbiology and Immunology, University of Fribourg, Fribourg, Switzerland

## OPEN ACCESS

### Edited by:

Alexandre M. Carmo,  
Universidade do Porto, Portugal

### Reviewed by:

Nicole Boucheron,  
Medical University of Vienna, Austria  
Jacques A. Nunes,  
INSERM U1068 Centre de Recherche  
en Cancérologie de Marseille (CRCM),  
France

### \*Correspondence:

Jens V. Stein  
jens.stein@unifr.ch

### Specialty section:

This article was submitted to  
T Cell Biology,  
a section of the journal  
Frontiers in Immunology

Received: 28 May 2021

Accepted: 19 August 2021

Published: 09 September 2021

### Citation:

Thelen F, Wissmann S, Ruef N and  
Stein J V (2021) The Tec Kinase Itk  
Integrates Naïve T Cell Migration  
and *In Vivo* Homeostasis.  
Front. Immunol. 12:716405.  
doi: 10.3389/fimmu.2021.716405

Naïve T cells ( $T_N$ ) constitutively recirculate through secondary lymphatic organs (SLOs), where they scan dendritic cells (DCs) for cognate peptide-loaded major histocompatibility complexes (pMHC). Continuous trafficking between SLOs not only enables rapid clonal selection but also ensures  $T_N$  homeostasis by providing access to pro-survival signals from TCR, IL-7R, and the chemokine receptor CCR7. Inside the lymphoid tissue, CCR7-mediated  $T_N$  motility is mainly driven by the Rac activator DOCK2, with a separate contribution by a phosphoinositide-3-kinase  $\gamma$  (PI3K $\gamma$ )-dependent pathway. Tec tyrosine kinases and the Rac activator Tiam1 constitute prominent downstream effectors of PI3K signaling. Yet, the precise role of Tec kinase versus Tiam1 signaling during CCR7-mediated  $T_N$  migration and homeostasis remains incompletely understood. Here, we examined the function of the Tec family member interleukin-2-inducible T-cell kinase (Itk) and Tiam1 during  $T_N$  migration *in vitro* and *in vivo* using intravital microscopy. Itk deficiency caused a mild decrease in CCR7-triggered  $T_N$  migration, mirroring observations made with PI3K $\gamma$ <sup>-/-</sup> T cells, while lack of Tiam1 did not affect  $T_N$  motility. *In silico* modeling suggested that reduced migration in the absence of Itk does not result in a substantial decrease in the frequency of  $T_N$  encounters with DCs within the lymphoid tissue. In contrast, Itk was important to maintain *in vivo* homeostasis of CD4<sup>+</sup>  $T_N$ , also in MHCII-deficient hosts. Taken together, our data suggest that Itk contributes to  $T_N$  migration and survival by integrating chemokine receptor and TCR signaling pathways.

**Keywords:** T cell trafficking, chemokine, signal transduction, Tec kinase, CCL21/CCR7 axis, intravital 2-photon microscopy

## INTRODUCTION

Naïve T cells ( $T_N$ ) continuously roam secondary lymphoid organs (SLOs) including peripheral lymph nodes (PLNs) to scan for the presence of cognate peptide-loaded major histocompatibility complex (pMHC) on dendritic cells (DCs). The chemokine receptor CCR7 on  $T_N$  and its ligands CCL19 and CCL21 expressed by SLO stromal cells fulfill a key function in this process (1). CCL21 is central for recruitment of blood-borne  $T_N$  via high endothelial venules into the PLN parenchyma (2), where CCR7 ligands contribute to fast  $T_N$  motility of  $\sim 15 \mu\text{m}/\text{min}$  on a scaffold of fibroblastic reticular cells (FRCs) (3–7). This process enables efficient  $T_N$  scanning of pMHC presented on DC

surfaces (8, 9). In addition to providing an “antigen library” that mirrors the immune status of their surveilled area, SLOs provide critical factors for  $T_N$  homeostasis. First, FRCs are a main source of the prosurvival cytokine IL-7 (10). Second, tonic signaling by self-pMHC binding to the T cell receptor (TCR) on migrating T cells induces a baseline phosphorylation of the TCR complex  $\zeta$ ; chain important for responsiveness to foreign pMHC (11) and  $CD4^+$  T cell survival (12, 13). Third, CCR7 ligands themselves constitute prosurvival signals for circulating  $T_N$  (10). Accordingly, the expression of CCR7, the PLN homing receptor CD62L, and the IL-7 receptor CD127 are transcriptionally coordinated in  $T_N$  (14).

On a molecular level, CCR7 activation triggers an increase in F-actin polymerization, mainly *via* the Rac guanine exchange factor (GEF) DOCK2 that catalyzes the formation of Rac-GTP at the cell’s leading edge. This, in turn, activates the actin nucleator Arp2/3 complex *via* the nucleation promoting factor Scar/WAVE (15, 16). DOCK2-Rac-Scar/WAVE-Arp2/3-driven retrograde (i.e., from the cell front to the rear) F-actin flow imprints the characteristic amoeboid shape of migrating  $T_N$  and forms the basis for rapid cellular translocation by force-coupling of cortical actin to the extracellular substrate *via* transmembrane receptors, mainly LFA-1 (17).

In addition to DOCK2 activation, chemokine receptors activate a phosphoinositide-3-kinase (PI3K) pathway in T cells (18). In  $T_N$ , CCR7 signaling activates the p110 $\gamma$  isoform through its interaction with G $\beta\gamma$  subunits that dissociate from G $\alpha_i$  after ligand binding (19). While pharmacological or genetic inhibition of this pathway does not affect the major DOCK2-Rac-Arp2/3 axis, PI3K blockade induces a minor but significant decrease in  $T_N$  migration *in vitro* and *in vivo* (19, 20). To date, the downstream signals that transmit PI3K signals for CCR7-mediated  $T_N$  migration remain incompletely understood. PI3K-generated phosphoinositide-3,4,5-triphosphate (PIP3) at the inner plasma membrane is recognized by proteins containing pleckstrin homology (PH) domains, such as the Rac GEF Tiam1, which has been implicated in T cell trafficking (21, 22). Additionally, Tec proteins constitute a well-characterized PH-domain-containing nonreceptor tyrosine kinase family that plays key regulatory functions in lymphocyte development, activation, and effector differentiation. The Tec family is composed of five members, of which Itk and Rlk are expressed in  $T_N$  (23). Itk signals from multiple surface receptors, such as TCR, the costimulatory receptor CD28, and chemokine receptors (23–25). In accordance with this, Itk-deficient and Itk/Rlk double-deficient T cells show reduced chemotaxis to CXCL12 (26, 27). Itk activation of Vav1, a GEF for the small GTPases Rac1 and Cdc42, is important for actin reorganization and adhesion (23, 28–30). Yet, the precise roles of Itk and Tiam1 during CCR7-triggered DOCK2- versus PI3K-dependent  $T_N$  migration and their impact on physiological  $T_N$  motility and homeostasis have not been assigned thus far.

Here, we investigated the role of Itk and Tiam1 in CCR7-driven  $T_N$  motility and survival after adoptive transfer. Our data uncover a role for Itk but not Tiam1 downstream PI3K-dependent *in vitro*  $T_N$  polarization and migration in response

to the CCR7 ligand CCL21, with a concomitant decrease in homing capacity to SLOs. While intravital imaging confirmed that *in vivo* T cell motility is reduced in the absence of Itk, *in silico* track modeling suggests only a minor impact on the efficacy to encounter DCs in the LN parenchyma. In contrast, significantly fewer Itk-deficient  $CD4^+$  T cells were recovered from blood and SLOs 8–14 days after adoptive transfer into WT and MHCII-deficient recipients, supporting a role for this Tec family member for  $T_N$  homeostasis even in the absence of tonic TCR signaling.

## RESULTS

### CCL21-Induced T Cell Polarization and Migration Are Impaired in the Absence of Itk

We first examined the impact of Itk deficiency on CCR7-triggered rapid F-actin polymerization. Akin to PI3K $\gamma^{-/-}$  T cells (19), we detected a small but consistent reduction of F-actin polymerization in Itk $^{-/-}$  T cells immediately after CCL21 addition (**Figures 1A, B**). This difference disappeared when WT cells were pretreated with Wortmannin (Wn), a broad PI3K inhibitor, whereas the same treatment on Itk $^{-/-}$  cells caused no further decrease in F-actin polymerization (**Figures 1A, B**). This is in line with results showing that Itk acts downstream of PI3K and contributes to F-actin polymerization upon chemokine receptor activation in T cells (23). Given the close causal relation between F-actin treadmilling and T cell shape (17), we examined the impact of Itk on chemokine-induced polarization. T cells were allowed to adhere to fibronectin-coated glass slides and stimulated with CCL21 for 20 min, followed by immunofluorescent analysis of PKC $\zeta$  and CD44 as markers for leading edge and uropod, respectively (**Figure 1C**). Itk $^{-/-}$  T cells showed reduced cellular polarization as compared to WT T cells and resembled PI3K $\gamma^{-/-}$  T cells or WT T cells treated with the pan-PI3K inhibitor Wortmannin (Wn) (**Figure 1D**). Taken together, our data suggest that a PI3K-Itk pathway contributes to F-actin polymerization and T cell polarization upon stimulation with CCR7 ligands.

Itk $^{-/-}$  mice display a defect in thymic positive selection and show an increased ratio of “memory-like” CD44<sup>high</sup> to CD44<sup>low</sup>  $T_N$  in SLOs (31, 32) (**Figure S1A**). To exclude this as cause of reduced Itk $^{-/-}$  T cell response to CCL21, we enriched CD62L<sup>high</sup>CD44<sup>low</sup> *bona fide*  $T_N$  by depleting CD44<sup>high</sup> T cells using titrated amounts of anti-CD44 mAb-coated magnetic beads as described (33) and applied bead sorting to both WT and Itk $^{-/-}$  T cells (**Figure S1B**). As reported for migration to CXCL12 (26, 27), *bona fide* Itk $^{-/-}$   $T_N$  migration toward increasing concentrations of CCL21 showed a minor but significant and consistent reduction (**Figure 1E**).

In contrast to Itk, DOCK2 activity in lymphocytes is regulated in a PI3K-independent manner (19) and plays a pivotal role in chemokine-induced migration (15). Accordingly, we observed reduced migration of both WT and Itk $^{-/-}$   $T_N$  with the specific DOCK2 inhibitor CPYPP (34) in a dose-dependent manner

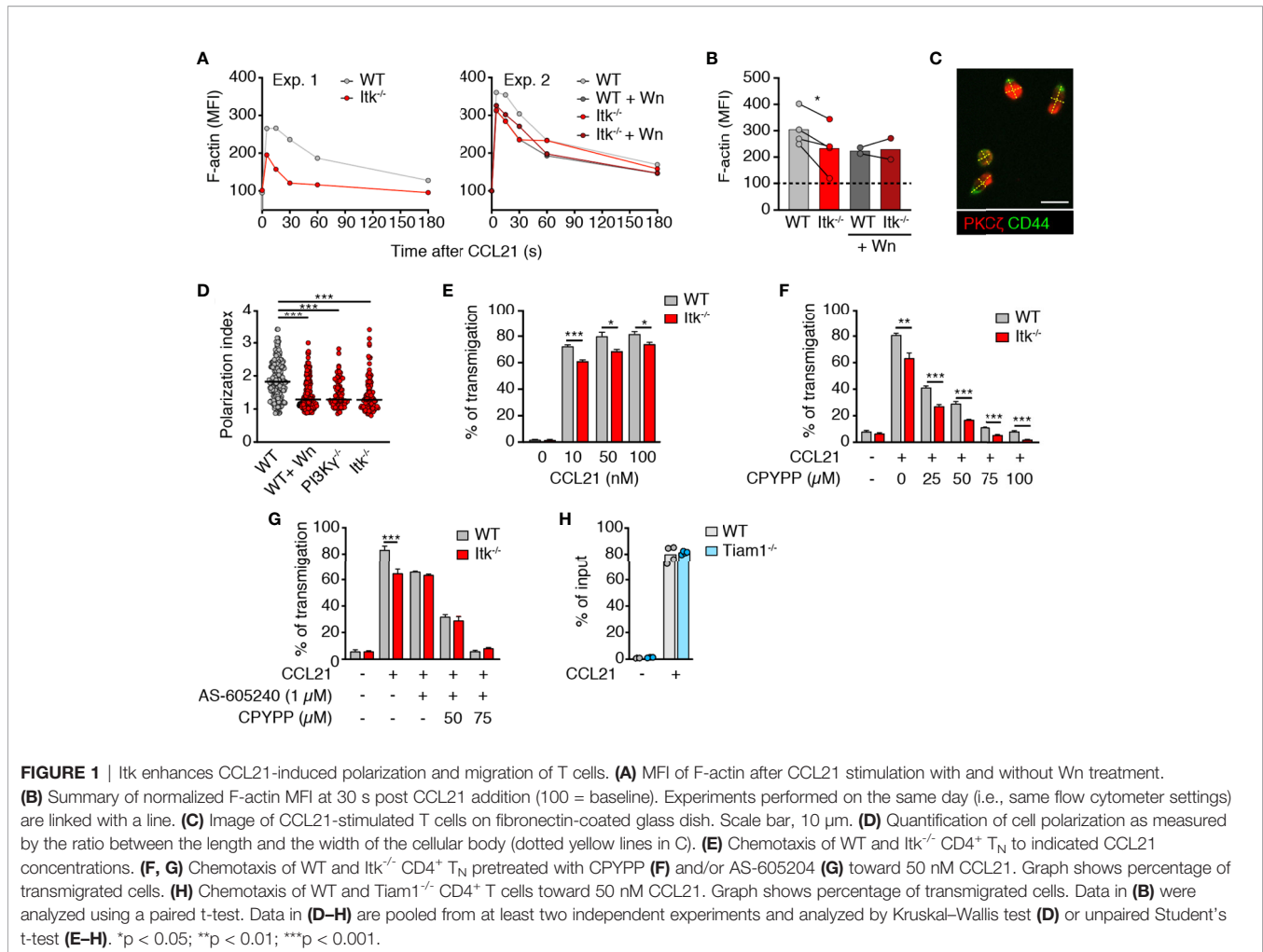


(Figure 1F). The migratory difference between WT and *Itk*<sup>-/-</sup> CD4<sup>+</sup> T cells was maintained during CPYPP treatment, confirming that Itk-dependent migration is uncoupled from DOCK2-induced motility. In line with this, treatment of WT CD4<sup>+</sup> T<sub>N</sub> with the specific PI3K $\gamma$  inhibitor AS-605240 reduced migration to the same level as of *Itk*<sup>-/-</sup> CD4<sup>+</sup> T<sub>N</sub>, while this treatment did not have an impact on *Itk*<sup>-/-</sup> CD4<sup>+</sup> T<sub>N</sub> chemotaxis (Figure 1G). Consistent with the abolished chemotaxis of DOCK2 x PI3K $\gamma$ -double deficient T cells (19), combined CPYPP + AS-605240 treatment completely abrogated T<sub>N</sub> migration to CCL21 (Figure 1G). Similarly, migration toward CXCL12 was partially reduced in WT T<sub>N</sub> by either CPYPP or AS-605240 treatment, while combined CPYPP + AS-605240 treatment abolished T<sub>N</sub> chemotaxis (Figure 1S1C). In contrast, *Itk*<sup>-/-</sup> T<sub>N</sub> migration to CXCL12 was not affected by AS-605240, whereas CPYPP treatment severely impaired chemotaxis toward CXCL12 (Figure 1S1C). These data suggested that the dual engagement of DOCK2- and PI3K $\gamma$ -dependent signaling affects other chemokine receptors as well. Inhibitor treatment did not affect the viability of T<sub>N</sub>, as assessed by PI staining (>90% viability after double inhibitor treatment).

Itk has been reported to be constitutively associated with the Rac/Cdc42 GEF Vav1, which mediates its effects on the actin cytoskeleton (30). In addition to Vav1, the Rac GEF Tiam1 becomes activated downstream of PI3K signaling (35), and Tiam1 has been previously shown to mediate T cell polarization and migration to CXCL12 and CCL21 via the Par complex (22, 36). We therefore examined whether *Tiam1*<sup>-/-</sup> T cells were impaired in their motility to CCL21. However, *Tiam1*<sup>-/-</sup> CD4<sup>+</sup> T cells showed no defect in chemotaxis (Figure 1H). Taken together, these results confirm that DOCK2 plays a dominant function in CCL21-dependent T<sub>N</sub> migration, while a PI3K $\gamma$ -Itk axis contributes to optimal cell polarity and chemokine responsiveness, potentially by regulating the activity of Vav1 or other GEFs.

## Itk Supports T<sub>N</sub> Migration in LN Parenchyma

Rlk/Itk-double-deficient naïve T cells display impaired *in vivo* homing to spleen and PLNs (27). We confirmed this observation after adoptive transfer of WT and *Itk*<sup>-/-</sup> CD4<sup>+</sup> T<sub>N</sub>, since we recovered fewer *Itk*-deficient T cells in spleen and other SLOs at

2 h post transfer, while these cells were more abundant in blood (Figure 2A). Since CCR7 contributes to  $T_N$  motility inside the LN parenchyma (3, 5, 6, 17, 37), we set out to assess the impact of Itk deficiency on *in vivo* T cell scanning behavior. We adoptively transferred fluorescently labeled  $CD4^+$  WT and  $Itk^{-/-}$   $T_N$  into C57BL/6 recipients and performed intravital imaging of the popliteal LN 16–24 h post transfer. We detected a minor but significant reduction in  $Itk^{-/-}$   $CD4^+$  versus WT  $T_N$  speeds ( $13.2 \pm 0.3$  and  $11.9 \pm 0.3$   $\mu\text{m}/\text{min}$  for WT and  $Itk^{-/-}$   $T_N$ , respectively; mean  $\pm$  SEM; Figure 2B) without affecting the turning angles as a readout for directionality (38) (Figure 2C). As a result, the motility coefficient (MC), which represents a measure of the average scanned area per time, was reduced from  $64$   $\mu\text{m}^2/\text{min}$  for WT to  $36$   $\mu\text{m}^2/\text{min}$  for  $Itk^{-/-}$   $CD4^+$   $T_N$  (Figure 2D). In contrast, parenchymal  $CD4^+$  T cell speeds were unaffected by Tiam1 deficiency (Figure 2E), in line with *in vitro* chemotaxis data.

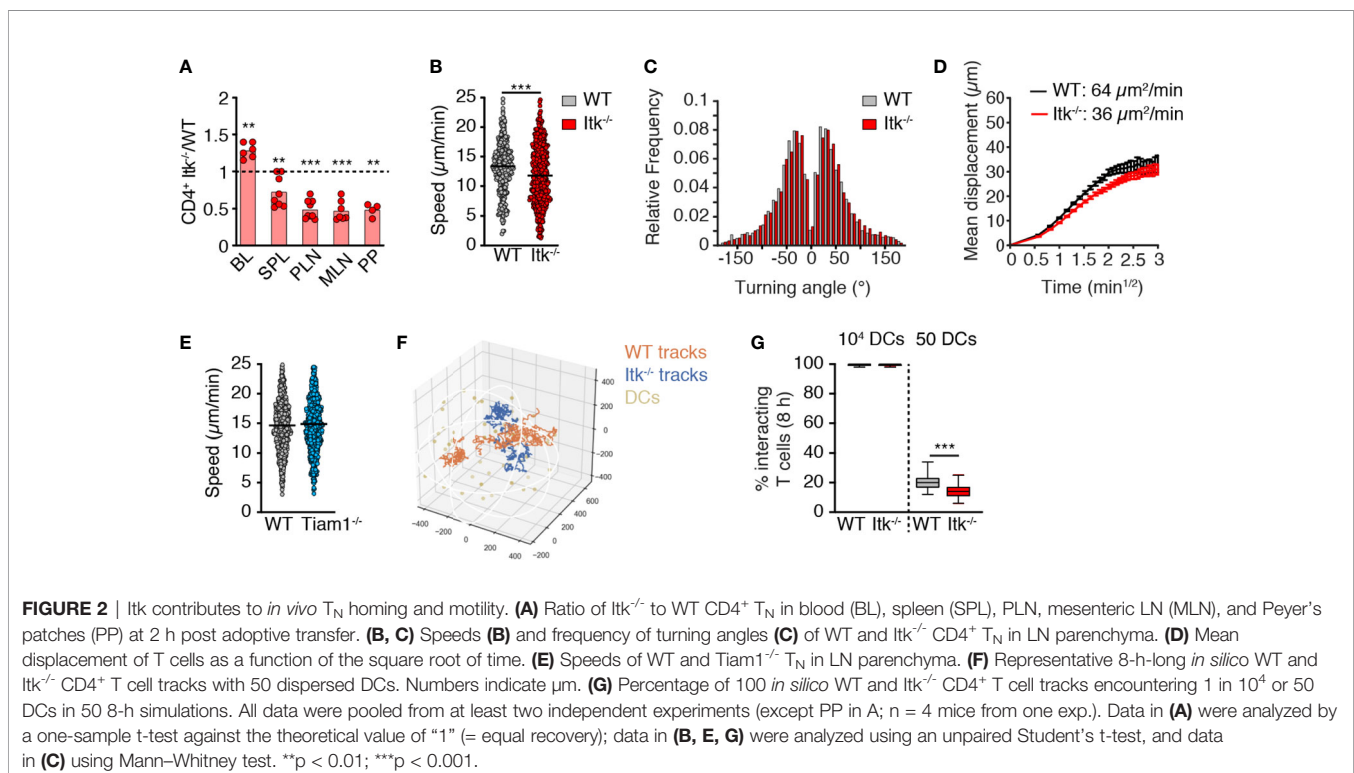
Based on the measured *in vivo* motility data, we modeled how  $T_N$  encounters with abundant ( $10^4$ ) or rare (50) DCs would be affected by Itk deficiency using *in silico* generated tracks in an artificial 3D volume representing the T cell zone (39) (Figure 2F). Both cell types efficiently intercepted highly abundant DCs (Figure 2G). In contrast to the reported reduction of T cell–DC encounters in the absence of DOCK2 (39), the absence of Itk only had a minor impact on the ability of migrating  $T_N$  to encounter rare cognate pMHC-bearing DCs ( $20.1 \pm 4.9\%$  and  $13.8 \pm 4.3\%$  of WT and  $Itk^{-/-}$  *in silico* T cell tracks, respectively, engaging in DC encounters in 8-h simulations with a total of 50 DCs/T cell zone; mean  $\pm$  SD; Figure 2G). Taken together, Itk signaling makes a minor but

detectable contribution to *in vivo* T cell migration akin to observations made with  $PI3K\gamma^{-/-}$  T cells (40), yet without causing a substantial decrease in the likelihood of T cell–DC encounters.

## Itk Contributes to Circulating $T_N$ Homeostasis

$CD4^+$   $T_N$  continuously homes to SLO to receive pro-survival factors provided in part by TCR and CCR7 signaling. We therefore investigated whether Itk promotes  $T_N$  homeostasis by facilitating homing and integration of pro-survival signals from pMHC and/or CCR7. We transferred fluorescently labeled WT and  $Itk^{-/-}$   $CD4^+$   $T_N$  at a 1:1 ratio into age- and sex-matched recipients as described (10). After 10–14 days, we isolated SLOs and blood to determine the ratio of recovered WT and  $Itk^{-/-}$   $CD4^+$   $T_N$  (Figure 3A). In all organs tested, we detected an approximately 30% reduction in the frequency of  $CD4^+$   $T_N$  lacking  $Itk^{-/-}$  expression in comparison to their WT counterparts (Figure 3B). In contrast to the short-term homing experiment (Figure 2A), we now observed fewer  $Itk^{-/-}$   $T_N$  in blood as compared to their WT counterparts. In contrast, we recovered a similar ratio of Tiam1 $^{-/-}$ : WT T cells from all tissues at 14 days post transfer (Figure 3C).

To examine whether reduced recovery of  $Itk^{-/-}$  T cells is owing due to impaired homeostatic TCR signaling (24), we transferred  $Itk^{-/-}$  and WT  $CD4^+$   $T_N$  into MHCII $^{-/-}$  recipients in a 1:1 ratio as above. On 8 days post transfer, we collected SLOs and measured the ratio of recovered WT:  $Itk^{-/-}$   $CD4^+$  T cells. Similar to WT recipients,  $Itk^{-/-}$   $CD4^+$   $T_N$  were underrepresented in blood and most SLOs except spleen (Figure 3D). Taken



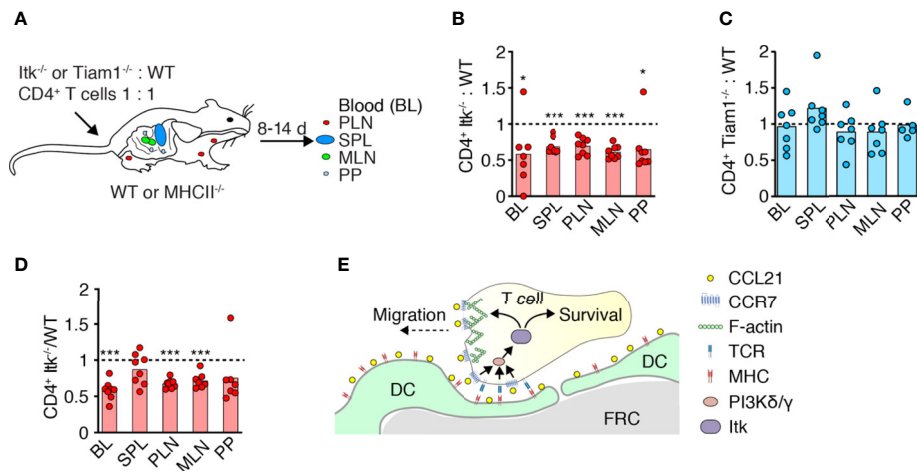


**FIGURE 3** | Itk supports physiological  $T_N$  homeostasis. **(A)** Experimental layout. Fluorescently labeled WT and Itk<sup>-/-</sup> or Tiam1<sup>-/-</sup> CD4<sup>+</sup>  $T_N$  were transferred in a 1:1 ratio into WT or MHCII<sup>-/-</sup> recipients, and blood (BL), spleen (SPL), PLN, mesenteric LN (MLN), and Peyer's patches (PP) were analyzed 8–14 days post transfer (p.t.) by flow cytometry. **(B–D)** Itk<sup>-/-</sup> or Tiam1<sup>-/-</sup> to WT CD4<sup>+</sup>  $T_N$  ratio recovered 10–14 days p.t. into WT **(B, C)** or 8 days p.t. into MHCII<sup>-/-</sup> recipients **(D)**, normalized to input. **(E)** Scheme of Itk function in  $T_N$  migration and survival. Data in **(B–D)** are from two independent experiments and analyzed by a one-sample t-test against the theoretical value of “1” (= equal recovery). \* $p < 0.05$ ; \*\*\* $p < 0.001$ .

together, these data suggest a role for Itk in mediating  $T_N$  homeostasis beyond TCR signal transduction, presumably by signal transmission *via* CCR7 or other chemoattractant receptors (**Figure 3E**).

## DISCUSSION

$T_N$  uses two separate signaling modules for CCR7-triggered motility, a major DOCK2-dependent and a minor PI3K $\gamma$ -dependent pathway (19, 40). While the DOCK2-Scar/WAVE-Arp2/3-Rac signaling cascade is well characterized, it has remained unclear which molecules act downstream PI3K after CCR7 activation. Here we report a role for the Tec kinase Itk in optimizing PI3K-dependent  $T_N$  polarization and migration. In line with the limited contribution of PI3K signaling for homeostatic  $T_N$  migration, we find that Itk deficiency had only a minor effect on CCR7-induced motility *in vitro* and  $T_N$  scanning behavior *in vivo*. In contrast, Itk deficiency impaired short-term  $T_N$  homing to SLOs and precipitated a loss of  $T_N$  recovery after 1–2 weeks post transfer. Thus, Itk integrates PI3K-dependent motility and homeostasis of circulating  $T_N$ .

Unlike in neutrophils (41), DOCK2 activation in T cells occurs independently of PIP3 and might involve additional phospholipids such as phosphatidic acid (42). Given that PI3K activation is a universal hallmark of chemokine receptors including CCR7 (18), there is, to date, remarkably little knowledge on the physiological impact of this pathway in primary T cells. Tec kinases act at the crossroads of TCR and chemokine receptor signaling and have well-characterized effects on the actin cytoskeleton in multiple cell types, with a wide-ranging impact on T cell development, activation, and

differentiation (23, 24). Here we focused on the role of Itk, since its activity is regulated by PIP3 binding to its PH domain, in contrast to the other Tec family member expressed in naïve T cells, Rlk (23) (**Figure S2**). While we identify a role for Itk in CCR7-triggered PI3K-dependent  $T_N$  migration, our findings suggest a more prominent role of Itk for long-term  $T_N$  survival. Our data further indicate that Itk-dependent homeostasis is not solely driven by TCR signaling, as evidenced by reduced recovery of Itk<sup>-/-</sup>  $T_N$  in MHC II-deficient hosts as compared to WT  $T_N$ . As TCR stimulates the PI3K $\delta$  isoform in T cells, while CCR7 activates PI3K $\gamma$ , Itk is in a key position to integrate both baseline PIP3 signals generated during homeostatic  $T_N$  recirculation into a prosurvival program (**Figure 3E**). One caveat is that the I-Aa<sup>-/-</sup> recipients we used as MHCII-deficient might still retain residual expression of noncanonical MHC molecules (12, 43).

In contrast to previous publications (22, 36), we were unable to assign a role for Tiam1 in CCR7-driven, PI3K-mediated  $T_N$  migration *in vitro* and *in vivo*. While the reason for this discrepancy might be due to the different mouse strain background used in both studies, our findings reflect the lack of Tiam1 expression in C57BL/6  $T_N$  (www.immgen.org). Similarly, Tiam2 was not expressed in naïve CD4<sup>+</sup> T cells (**Figure S2**). Furthermore, recent work suggests that the Tiam1 PH domain binds with a lower affinity to PIP3 as compared to other membrane lipids such as phosphoinositide-5-phosphate (44). Taken together, our data assign a role for Itk during CCR7-mediated signaling in T cells, leading to enhanced actin polymerization, polarization, and migration. Yet, the most relevant impact of Itk is in promoting  $T_N$  homeostasis, presumably by facilitating SLO homing and integration of prosurvival pMHC and CCR7 signals.

## MATERIAL AND METHODS

### Mouse Lines

C57BL/6 mice were purchased from Janvier labs. *Itk*<sup>-/-</sup> (31) and *Tiam1*<sup>-/-</sup> mice (45) were obtained from P. Schwartzberg (NIH, Bethesda, MD, USA) and J. van Buul (Sanquin Research Center, The Netherlands), respectively. *PI3Kγ*<sup>-/-</sup> and *H2-Aa*<sup>tm1Blt</sup> (*MHCII*<sup>-/-</sup>) were described (46, 47). Mice were bred at the Department of Clinical Research of the University of Bern and at the University of Fribourg. Experiments were approved by the Cantonal authorities and performed in accordance with the Swiss Federal Veterinary Office guidelines.

### T Cell Isolation

Spleens, PLNs, and mesenteric LNs (MLNs) were harvested and homogenized using a 70- $\mu$ m cell strainer and a syringe plug. T cells or CD4<sup>+</sup> T cells were isolated with an EasySep Mouse negative selection kit according to the manufacturer's protocol (STEMCELL Technologies). For depletion of CD44<sup>high</sup> CD4<sup>+</sup> T cells, 2.5  $\mu$ g of biotinylated anti-CD44 mAb (BD Biosciences) was added per 10<sup>7</sup> cells. Cells were incubated for 20 min on ice. CD44<sup>low</sup> *bona fide* T<sub>N</sub> was negatively isolated using an EasySep<sup>TM</sup> Streptavidin RapidSpheres<sup>TM</sup> Isolation kit according to the manufacturer's protocol (STEMCELL Technologies). Purity was typically >95%.

### Flow Cytometry

Single cell suspensions from SLOs were isolated and homogenized using 70- $\mu$ m cell strainers. Fc receptors were blocked with purified anti-CD16/CD32 mAb (2.4G2) in a FACS buffer (PBS with 1% FCS and 0.05% NaN<sub>3</sub>) for 10 min. Cells were stained with fluorochrome-conjugated mAbs against CD8 (53-6.7), CD62L (Mel-14; 4°C for 30 min), CD4 (RM4-5; all Biolegend), and CD44 (IM7; BD Bioscience) with appropriate isotype controls and analyzed by flow cytometry (BD Biosciences).

### F-Actin Polymerization, Cell Polarization, and Chemotaxis

For F-actin polymerization, T cells from *Itk*<sup>-/-</sup>, *PI3Kγ*<sup>-/-</sup>, and WT mice were starved for 1.5 h in a serum-free medium. Where noted, cells were pretreated with 0.5  $\mu$ M Wortmannin (Calbiochem) for 1 h at 37°C. CCL21 (100 nM; Peprotech) was added to 2 x 10<sup>6</sup> cells/ml in a 37°C water bath, and cells were fixed at indicated time points in 4% cold PFA. Cells were permeabilized and labeled with FITC-Phalloidin (Invitrogen) as described (19). For polarization assays, T cells were added on 1  $\mu$ g/ml fibronectin-coated glass slides before the addition of CCL21 (100 nM) and fixation after 20 min with 2% PFA. After permeabilization with 0.1% Triton X-100 (5 min), cells were incubated with anti-protein kinase  $\zeta$ ; (PKC $\zeta$ ) (H-1; Santa Cruz Biotechnology) and biotin-labeled anti-CD44 (IM7; BD Pharmingen) mAbs. Primary antibodies were detected with a Cy3-labeled anti-mouse Ab (Jackson ImmunoResearch Laboratories) and Alexa488-labeled avidin (Molecular Probes). For chemotaxis assays, T<sub>N</sub> was pretreated with inhibitors

for DOCK2 (CPYPP) and *PI3Kγ* (AS-605240; both Tocris) as indicated for 1 h at 37°C, and 0.5 x 10<sup>6</sup> T<sub>N</sub>/well were added to Transwell chambers (5- $\mu$ m pore size; Costar) to migrate to 50 nM CCL21 for 1.5 h at 37°C in the presence of the inhibitors. Cell viability was assessed by PI staining at the end of the experiment. Input and migrated T cells were enumerated by flow cytometry.

### Intravital Microscopy of Popliteal LN

(5-(and-6)-((4-chloromethyl) benzoyl) amino) tetramethylrhodamine (CMTMR, CellTracker orange) and Chloromethyl-coumarin (CMAC, CellTracker blue)-labeled WT, *Itk*<sup>-/-</sup> or *Tiam1*<sup>-/-</sup> CD4<sup>+</sup> T<sub>N</sub> (3 x 10<sup>6</sup>) were injected i.v. into sex-matched C57BL/6 mice 24–32 h prior to imaging. The right popliteal LN of recipient mice was surgically prepared as previously described (48). 2PM imaging was performed using a TrimScope 2PM system (LaVision Biotec) and a 20X objective (NA 0.95; Olympus). 16-slice z stacks with 4- $\mu$ m spacing of 250 x 250  $\mu$ m field of views were acquired every 20 s for 20 min. Imaging was performed in the T cell zone as identified by the presence of high endothelial venules (labeled with Alexa Fluor 633-coupled MECA-79; 10  $\mu$ g/mouse). Volocity software (PerkinElmer) was used to generate volume-rendered 4D movies and for semiautomated tracking of cell motility. Mean single cell track speeds were calculated from the x,y,z coordinates of cell centroids using Matlab (The MathWorks) (49).

### Estimation of T Cell–DC Encounters

We simulated 200 8-h-long WT and *Itk*<sup>-/-</sup> T cell tracks by sampling from control and *Itk*<sup>-/-</sup> T cell tracks acquired by 2PM. As steps at higher velocities tend to have smaller turning angles, we drew combinations of speed, turning angle, and plane angle from the same step instead of drawing speed, turning angle, and plane angle separately. To additionally account for the correlation of velocity and turning angle, we repeatedly exchanged random steps of our samples, keeping only those exchanges that made the mean squared differences of consecutive speeds and turning angles of our synthetic track more similar to the same means of the measured tracks. We stopped exchanging when both means of the simulated track were smaller than those of the measured tracks. To simulate contact formation among a predefined number of synthetic T cells and a number of DCs, we randomly chose 100 simulated T cell tracks and moved them to starting positions normally distributed around the center of a spherical T cell zone of 1-mm diameter for 8 h as described (39). We chose the SD of 150  $\mu$ m, such that half of the WT tracks resided within the T cell zone for an average half-life of 11 h (40). We considered all steps of the track within the T cell zone, including reentry as residency time. We then checked, step by step, the distance to 10'000 and 50 static DCs uniformly distributed throughout the T cell zone. We considered proximity  $\geq$  15  $\mu$ m as a stable contact and did not allow T cells to move on. We repeated the different simulations 50 times to obtain stable distributions of outcomes. This analysis was performed using open Python libraries for scientific computing (<https://github.com/germannp/lambda/blob/master/lambda/>).

## In Vivo Homing and Homeostasis

WT, *Itk*<sup>-/-</sup>, or *Tiam1*<sup>-/-</sup> T<sub>N</sub> were labeled with Carboxyfluorescein succinimidyl ester (CFSE; Life Technologies) or eFluor 670 (e670; Life Technologies) for 15–20 min at 37°C in PBS, with dyes swapped between experiments, and 3 × 10<sup>6</sup> cells of each were injected i.v. at a 1:1 ratio into 5- to 10-week-old C57BL/6J or MHCII<sup>-/-</sup> recipient mice. At the indicated time points, blood and SLOs were isolated and analyzed by flow cytometry for percentage of transferred cells among CD4<sup>+</sup> T cells. In WT recipients, we recovered between 0.22% (in PP) and 1.84% (in blood) of WT and *Itk*<sup>-/-</sup> CD4<sup>+</sup> T cells at 10 to 14 days post transfer, while in MHCII<sup>-/-</sup> recipients, we recovered between 0.98% (in PP) and 8.37% (in blood) of transferred cells at 8 days post transfer.

## Statistical Analysis

Data were analyzed using Prism (GraphPad Software) using unpaired Student's t-test or Mann–Whitney or Kruskal–Wallis tests. P-values < 0.05 were considered significant.

## DATA AVAILABILITY STATEMENT

The original contributions presented in the study are included in the article/**Supplementary Material**. Further inquiries can be directed to the corresponding author.

## ETHICS STATEMENT

The animal study was reviewed and approved by Kanton of Bern and Fribourg Amt für Lebensmittelsicherheit und Veterinärwesen.

## AUTHOR CONTRIBUTIONS

FT performed the experiments and analyzed the data with the help of SW. NR performed *in silico* analysis. JS designed the

experiments, analyzed the data, and wrote the manuscript with input from all coauthors. All authors contributed to the article and approved the submitted version.

## FUNDING

This work was funded by Swiss National Foundation (SNF) project grant 31003A\_172994 and 310030-200406 and Sinergia project CRSII5\_170969 (to JS).

## ACKNOWLEDGMENTS

We thank Federica Moalli, Bettina Stolp, Philipp Germann, and Varsha Kumar for help with experiments and Yağmur Farsakoğlu for critical reading.

## SUPPLEMENTARY MATERIAL

The Supplementary Material for this article can be found online at: <https://www.frontiersin.org/articles/10.3389/fimmu.2021.716405/full#supplementary-material>

**Supplementary Figure 1** | CD44<sup>high</sup> CD4<sup>+</sup> T cell depletion and migration to CXCL12. **(A)** Representative flow cytometry plot showing CD44 and CD62L expression on WT and *Itk*<sup>-/-</sup> CD4<sup>+</sup> and CD8<sup>+</sup> T cells. Numbers indicate percentage. **(B)** Representative flow cytometry plot of CD44 and CD62L expression on CD4<sup>+</sup> T cells before and after negative isolation with CD44-coated beads. **(C)** Chemotaxis of WT and *Itk*<sup>-/-</sup> CD4<sup>+</sup> T<sub>N</sub> treated with either CPYPP and/or AS-605204 towards 100 nM CXCL12. Graph shows percentage of transmigrated cells. Data in C were analyzed using an unpaired t-test and pooled from two independent experiments. \*p < 0.05; \*\*\*p < 0.001.

**Supplementary Figure 2** | RNAseq expression level of *Tec*, *Tiam* and *Vav* family members in spleen CD4<sup>+</sup> T<sub>N</sub>. Data are from Immgen database ([www.immgen.org](http://www.immgen.org)).

## REFERENCES

- Förster R, Davalos-Misslitz AC, Rot A. CCR7 and Its Ligands: Balancing Immunity and Tolerance. *Nat Rev Immunol* (2008) 8:362–71. doi: 10.1038/nri2297
- Stein JV, Rot A, Luo Y, Narasimhaswamy M, Nakano H, Gunn MD, et al. The CC Chemokine Thymus-Derived Chemotactic Agent 4 (TCA-4, Secondary Lymphoid Tissue Chemokine, 6Ckine, Exodus-2) Triggers Lymphocyte Function-Associated Antigen 1-Mediated Arrest of Rolling T Lymphocytes in Peripheral Lymph Node High Endothelial Venules. *J Exp Med* (2000) 191:61–76. doi: 10.1084/jem.191.1.61
- Woolf E, Grigorova I, Sagiv A, Grabovsky V, Feigelson SW, Shulman Z, et al. Lymph Node Chemokines Promote Sustained T Lymphocyte Motility Without Triggering Stable Integrin Adhesiveness in the Absence of Shear Forces. *Nat Immunol* (2007) 8:1076–85. doi: 10.1038/ni1499
- Krummel MF, Bartumeus F, Gérard A. T Cell Migration, Search Strategies and Mechanisms. *Nat Rev Immunol* (2016) 16:193–201. doi: 10.1038/nri.2015.16
- Okada T, Cyster JG. CC Chemokine Receptor 7 Contributes to Gi-Dependent T Cell Motility in the Lymph Node. *J Immunol* (2007) 178:2973–8. doi: 10.4049/jimmunol.178.5.2973
- Worbs T, Mempel TR, Bölter J, Andrian von UH, Förster R. CCR7 Ligands Stimulate the Intranasal Motility of T Lymphocytes *In Vivo*. *J Exp Med* (2007) 204:489–95. doi: 10.1084/jem.20061706
- Bajénoff M, Egen JG, Koo LY, Laugier JP, Brau F, Glaichenhaus N, et al. Stromal Cell Networks Regulate Lymphocyte Entry, Migration, and Territoriality in Lymph Nodes. *Immunity* (2006) 25:989–1001. doi: 10.1016/j.immuni.2006.10.011
- Katakai T, Habiro K, Kinashi T. Dendritic Cells Regulate High-Speed Interstitial T Cell Migration in the Lymph Node via LFA-1/ICAM-1. *J Immunol* (2013) 191:1188–99. doi: 10.4049/jimmunol.1300739
- Moreau HD, Bogle G, Bouso P. A Virtual Lymph Node Model to Dissect the Requirements for T-Cell Activation by Synapses and Kinapses. *Immunol Cell Biol* (2016) 94:680–8. doi: 10.1038/icb.2016.36
- Link A, Vogt TK, Favre S, Britschgi MR, Acha-Orbea H, Hinz B, et al. Fibroblastic Reticular Cells in Lymph Nodes Regulate the Homeostasis of Naive T Cells. *Nat Immunol* (2007) 8:1255–65. doi: 10.1038/ni1513
- Štefanová I, Dorfman JR, Germain RN. Self-Recognition Promotes the Foreign Antigen Sensitivity of Naive T Lymphocytes. *Nature* (2002) 420:429–34. doi: 10.1038/nature01146
- Martin B, Bécourt C, Bienvenu B, Lucas B. Self-Recognition is Crucial for Maintaining the Peripheral CD4<sup>+</sup> T-Cell Pool in a Nonlymphopenic Environment. *Blood* (2006) 108:270–7. doi: 10.1182/blood-2006-01-0017
- Boyman O, Krieg C, Homann D, Sprent J. Homeostatic Maintenance of T Cells and Natural Killer Cells. *Cell Mol Life Sci* (2012) 69:1597–608. doi: 10.1007/s00018-012-0968-7

14. Kerdiles YM, Beisner DR, Tinoco R, Dejean AS, Castrillon DH, DePinho RA, et al. Foxo1 Links Homing and Survival of Naive T Cells by Regulating L-Selectin, CCR7 and Interleukin 7 Receptor. *Nat Immunol* (2009) 10:176–84. doi: 10.1038/ni.1689
15. Fukui Y, Hashimoto O, Sanui T, Oono T, Koga H, Abe M, et al. Haematopoietic Cell-Specific CDM Family Protein DOCK2 Is Essential for Lymphocyte Migration. *Nature* (2001) 412:826–31. doi: 10.1038/35090591
16. Goley ED, Welch MD. The ARP2/3 Complex: An Actin Nucleator Comes of Age. *Nat Rev Mol Cell Biol* (2006) 7:713–26. doi: 10.1038/nrm2026
17. Hons M, Kopf A, Hauschild R, Leithner A, Gaertner F, Abe J, et al. Chemokines and Integrins Independently Tune Actin Flow and Substrate Friction During Intranodal Migration of T Cells. *Nat Immunol* (2018) 19:606–16. doi: 10.1038/s41590-018-0109-z
18. Ward SG, Marelli-Berg FM. Mechanisms of Chemokine and Antigen-Dependent T-Lymphocyte Navigation. *Biochem J* (2009) 418:13–27. doi: 10.1042/BJ20081969
19. Nombela-Arrieta C, Lacalle RA, Montoya MC, Kunisaki Y, Megias D, Marqués M, et al. Differential Requirements for DOCK2 and Phosphoinositide-3-Kinase Gamma During T and B Lymphocyte Homing. *Immunity* (2004) 21:429–41. doi: 10.1016/j.immuni.2004.07.012
20. Stein JV, Soriano SF, M'Rini C, Nombela-Arrieta C, de Buitrago GG, Rodríguez-Frade JM, et al. CCR7-Mediated Physiological Lymphocyte Homing Involves Activation of a Tyrosine Kinase Pathway. *Blood* (2003) 101:38–44. doi: 10.1182/blood-2002-03-0841
21. Grönholm M, Jahan F, Marchesan S, Karvonen U, Aatonen M, Narumanchi S, et al. TCR-Induced Activation of LFA-1 Involves Signaling Through Tiam1. *J Immunol* (2011) 187:3613–9. doi: 10.4049/jimmunol.1100704
22. Gérard A, Mertens AEE, van der Kammen RA, Collard JG. The Par Polarity Complex Regulates Rap1- and Chemokine-Induced T Cell Polarization. *J Cell Biol* (2007) 176:863–75. doi: 10.1083/jcb.200608161
23. Gomez-Rodriguez J, Readinger JA, Viorritto IC, Mueller KL, Houghtling RA, Schwartzberg PL. Tec Kinases, Actin, and Cell Adhesion. *Immunol Rev* (2007) 218:45–64. doi: 10.1111/j.1600-065X.2007.00534.x
24. Andreotti AH, Schwartzberg PL, Joseph RE, Berg LJ. T-Cell Signaling Regulated by the Tec Family Kinase, Itk. *Cold Spring Harb Perspect Biol* (2010) 2:a002287. doi: 10.1101/cshperspect.a002287
25. Schwartzberg PL, Finkelstein LD, Readinger JA. TEC-Family Kinases: Regulators of T-Helper-Cell Differentiation. *Nat Publishing Group* (2005) 5:284–95. doi: 10.1038/nri1591
26. Fischer AM, Mercer JC, Iyer A, Ragin MJ, August A. Regulation of CXC Chemokine Receptor 4-Mediated Migration by the Tec Family Tyrosine Kinase Itk. *J Biol Chem* (2004) 279:29816–20. doi: 10.1074/jbc.M312848200
27. Takesono A, Horai R, Mandai M, Dombroski D, Schwartzberg PL. Requirement for Tec Kinases in Chemokine-Induced Migration and Activation of Cdc42 and Rac. *Curr Biol* (2004) 14:917–22. doi: 10.1016/j.cub.2004.04.011
28. Tybulewicz VLJ. Vav-Family Proteins in T-Cell Signalling. *Curr Opin Immunol* (2005) 17:267–74. doi: 10.1016/j.coi.2005.04.003
29. Vicente-Manzanares M. Control of Lymphocyte Shape and the Chemotactic Response by the GTP Exchange Factor Vav. *Blood* (2005) 105:3026–34. doi: 10.1182/blood-2004-07-2925
30. Dombroski D, Houghtling RA, Labno CM, Precht P, Takesono A, Caplen NJ, et al. Kinase-Independent Functions for Itk in TCR-Induced Regulation of Vav and the Actin Cytoskeleton. *J Immunol* (2005) 174:1385–92. doi: 10.4049/jimmunol.174.3.1385
31. Liao XC, Littman DR. Altered T Cell Receptor Signaling and Disrupted T Cell Development in Mice Lacking Itk. *Immunity* (1995) 3:757–69. doi: 10.1016/1074-7613(95)90065-9
32. Hu J, August A. Naive and Innate Memory Phenotype CD4+ T Cells Have Different Requirements for Active Itk for Their Development. *J Immunol* (2008) 180:6544–52. doi: 10.4049/jimmunol.180.10.6544
33. Köchl R, Thelen F, Vanes L, Brazão TF, Fountain K, Xie J, et al. WNK1 Kinase Balances T Cell Adhesion Versus Migration *In Vivo*. *Nat Immunol* (2016) 17:1075–83. doi: 10.1038/ni.3495
34. Nishikimi A, Uruno T, Duan X, Cao Q, Okamura Y, Saitoh T, et al. Blockade of Inflammatory Responses by a Small-Molecule Inhibitor of the Rac Activator DOCK2. *Chem Biol* (2012) 19:488–97. doi: 10.1016/j.chembiol.2012.03.008
35. Cain RJ, Vanhaesebroeck B, Ridley AJ. The PI3K P110alpha Isoform Regulates Endothelial Adherens Junctions via Pyk2 and Rac1. *J Cell Biol* (2010) 188:863–76. doi: 10.1083/jcb.200907135
36. Gérard A, van der Kammen RA, Janssen H, Ellenbroek SI, Collard JG. The Rac Activator Tiam1 Controls Efficient T-Cell Trafficking and Route of Transendothelial Migration. *Blood* (2009) 113:6138–47. doi: 10.1182/blood-2008-07-167668
37. Asperti-Boursin F, Real E, Bismuth G, Trautmann A, Donnadieu E. CCR7 Ligands Control Basal T Cell Motility Within Lymph Node Slices in a Phosphoinositide 3-Kinase-Independent Manner. *J Exp Med* (2007) 204:1167–79. doi: 10.1084/jem.20062079
38. Sumen C, Mempel TR, Mazo IB, Andrian von UH. Intravital Microscopy: Visualizing Immunity in Context. *Immunity* (2004) 21:315–29. doi: 10.1016/j.immuni.2004.08.006
39. Ackerknecht M, Gollmer K, Germann P, Ficht X, Abe J, Fukui Y, et al. Antigen Availability and DOCK2-Driven Motility Govern CD4+ T Cell Interactions With Dendritic Cells *In Vivo*. *J Immunol* (2017) 199:520–30. doi: 10.4049/jimmunol.1601148
40. Nombela-Arrieta C, Mempel TR, Soriano SF, Mazo I, Wymann MP, Hirsch E, et al. A Central Role for DOCK2 During Interstitial Lymphocyte Motility and Sphingosine-1-Phosphate-Mediated Egress. *J Exp Med* (2007) 204:497–510. doi: 10.1084/jem.20061780
41. Kunisaki Y, Nishikimi A, Tanaka Y, Takii R, Noda M, Inayoshi A, et al. DOCK2 Is a Rac Activator That Regulates Motility and Polarity During Neutrophil Chemotaxis. *J Cell Biol* (2006) 174:647–52. doi: 10.1083/jcb.200602142
42. Nishikimi A, Fukuhara H, Su W, Hongu T, Takasuga S, Mihara H, et al. Sequential Regulation of DOCK2 Dynamics by Two Phospholipids During Neutrophil Chemotaxis. *Science* (2009) 324:384–7. doi: 10.1126/science.1170179
43. Madsen L, Labrecque N, Engberg J, Dierich A, Svejgaard A, Benoist C, et al. Mice Lacking All Conventional MHC Class II Genes. *Proc Natl Acad Sci U S A* (1999) 96:10338–43. doi: 10.1073/pnas.96.18.10338
44. Viaud J, Lagarrigue F, Ramel D, Allart S, Chicanne G, Ceccato L, et al. Phosphatidylinositol 5-Phosphate Regulates Invasion Through Binding and Activation of Tiam1. *Nat Commun* (2014) 5:4080–17. doi: 10.1038/ncomms5080
45. Malliri A, van der Kammen RA, Clark K, van der Valk M, Michiels F, Collard JG. Mice Deficient in the Rac Activator Tiam1 are Resistant to Ras-Induced Skin Tumours. *Nature* (2002) 417:867–71. doi: 10.1038/nature00848
46. Hirsch E, Katanaev VL, Garlanda C, Azzolino O, Pirolo L, Silengo L, et al. Central Role for G Protein-Coupled Phosphoinositide 3-Kinase Gamma in Inflammation. *Science* (2000) 287:1049–53. doi: 10.1126/science.287.5455.1049
47. Köntgen F, Süs G, Stewart C, Steinmetz M, Bluethmann H. Targeted Disruption of the MHC Class II Aa Gene in C57BL/6 Mice. *Int Immunol* (1993) 5:957–64. doi: 10.1093/intimm/5.8.957
48. Moalli F, Cupovic J, Thelen F, Halbherr P, Fukui Y, Narumiya S, et al. Thromboxane A2 Acts as Tonic Immunoregulator by Preferential Disruption of Low-Avidity CD4+ T Cell-Dendritic Cell Interactions. *J Exp Med* (2014) 211:2507–17. doi: 10.1084/jem.20140137
49. Mempel TR, Henrickson SE, Andrian von UH. T-Cell Priming by Dendritic Cells in Lymph Nodes Occurs in Three Distinct Phases. *Nature* (2004) 427:154–9. doi: 10.1038/nature02238

**Conflict of Interest:** The authors declare that the research was conducted in the absence of any commercial or financial relationships that could be construed as a potential conflict of interest.

**Publisher's Note:** All claims expressed in this article are solely those of the authors and do not necessarily represent those of their affiliated organizations, or those of the publisher, the editors and the reviewers. Any product that may be evaluated in this article, or claim that may be made by its manufacturer, is not guaranteed or endorsed by the publisher.

Copyright © 2021 Thelen, Wissmann, Ruef and Stein. This is an open-access article distributed under the terms of the Creative Commons Attribution License (CC BY). The use, distribution or reproduction in other forums is permitted, provided the original author(s) and the copyright owner(s) are credited and that the original publication in this journal is cited, in accordance with accepted academic practice. No use, distribution or reproduction is permitted which does not comply with these terms.